A peer-reviewed version of this preprint was published in PeerJ on 9 April 2015.

View the peer-reviewed version (peerj.com/articles/892), which is the preferred citable publication unless you specifically need to cite this preprint.

Ganias K, Michou S, Nunes C. 2015. A field based study of swimbladder adjustment in a physostomous teleost fish. PeerJ 3:e892 https://doi.org/10.7717/peerj.892

Ganias Kostas[1], Nunes Cristina[2]

[1] School of Biology, Aristotle University of Thessaloniki, 54 124 Thessaloniki, Greece

[2] IPMA - Instituto Português do Mar e da Atmosfera, Avenida Brasília, s/n, 1449-006 Lisboa, Portugal

*Corresponding author

Tel: ++30 2310 998760

Fax: ++30 2310 998279

E-mail: kganias@bio.auth.gr

Abstract. The present study assesses swimbladder dynamics in natural occurring sardine, *Sardina pilchardus*, populations with the aim to examine whether this is affected by bathymetric positioning and the physiological state of the individuals. To do so swimbladder size and shape were modeled in relation to catch depth and the size of various visceral compartments such as gonad, liver, fat and stomach. Swimbladder size was shown to be related to depth in a way that individuals with smaller swimbladders occurred at larger depths. Moreover, evidence is provided that swimbladder in sardine might have a functional relationship both with the reproductive and the feeding state of individuals since none of the fish with hydrated gonads and/or large stomachs displayed distended swimbladders.

Introduction

In most marine teleosts the swimbladder provides a dual function, acting as a buoyancy regulating organ and as a gas reservoir for the acoustico-lateralis system (Nero et al., 2004); in a few species it may also function as an organ for sound production (e.g. oyster toadfish; Fine et al., 1995). Furthermore, the fish swimbladder is the main reflector of acoustic energy being responsible for up to 90-95% of the backscattered sound intensity which is of primary importance in acoustic estimates of fish abundance (Foote, 1980). As a corollary, mapping swimbladder structural morphology and understanding factors that may affect its size and shape is essential in quantifying its contribution to several biological functions such as buoyancy regulation and in improving accuracy in estimates of fish biomass from acoustic surveys.

To date most attempts to estimate swimbladder size have been performed by estimating its volume from the amount of gas it contains by means of gas colleting and measuring devices (e.g. Blaxter et al., 1979; Fine et al., 1995; Robertson et al., 2008). However, analysis of the structural morphology of the swimbladder needs more laborious techniques and specific equipment like the one described by Ona (1990) and Machias and Tsimenides (1995) who used photographs of parallel body slices to reconstruct the form of both swimbladder and other visceral compartments in order to accurately estimate their volume and shape. In another study Robertson et al. (2008) visualized and measured the size of zebrafish swimbladder by means of X-ray imagery.

Despite their accuracy the aforementioned methods are mostly designed to work under laboratory conditions which almost prohibits their use in field surveys and consequently in the

study of swimbladder dynamics in fish natural environment. The objective of the present work was to study swimbladder dynamics in wild populations of sardine, *Sardina pilchardus*. Sardine, in common with other clupeoids is a physostome and as such its swimbladder is not closed but connected to the anal opening and to the alimentary canal via a valved pneumatic duct (Blaxter et al., 1979). Due to this physiological specificity, sardine swimbladder may be subtle to volume modifications especially during its extensive diurnal vertical migrations (Zwolinski et al., 2007) due to significant changes in water pressure. In order to examine whether swimbladder dynamics in the Atlantic sardine is affected by bathymetric positioning and the physiological state of individuals we modeled the relationship of swimbladder size and shape with depth and the size of various visceral compartments.

Materials and methods

Sardine samples were collected off Portugal and the gulf of Cadiz in October 2008 and April 2009 within the remit of autumn/spring acoustic surveys carried out by the Portuguese Fisheries Research Institute (IPIMAR) (Table 1). All samples were collected using either a midwater or a bottom trawl with a vertical opening of ~10 m, towed at speeds of 3.5-4 knots for an average duration of 20 min. For each of the 10 samples used for the present analysis spatial coordinates, time, bottom and fishing depth were registered. In each haul, sardines were sorted out from the remaining catch and a sample was selected in a way that all length classes would be represented. These fish were subsequently measured for total length, L (mm), and total weight, W (0.1g), whilst maturity, fat index and stomach fullness were scored macroscopically.

Viscera were removed carefully to avoid possible damaging of the swimbladder and eviscerated body weight was also recorded. Subsequently, the coelomic cavity was carefully opened either manually or using forceps in order to expose the entire surface of the swimbladder (Fig. 1); swimbladders were scored macroscopically with respect to size (1: small; 2: medium; 3: large; 4: distended; Figs. 1a-d) and shape (1: normal-elliptical; 2: medially compressed; 3: compressed at the anterior region; 4: compressed at the posterior region) (Figs. 1e-g) and were subsequently photographed using a camera supported on a vertical plastic stand. This device provided easy adjustment of camera height to allow for quick and easy framing of specimens of different sizes and was essential to avoid vibrations and taking pictures at different angles. A ruler was always placed aside each specimen in order to calibrate scale in subsequent linear measurements. Gonads and liver from each fish were placed in plastic bags and frozen at -20^{0}C to be weighed (0.0001g) in the laboratory;

gonadosomatic and hepatosomatic indices were calculated using the formulas GSI=gonad weight/eviscerated weight*100 and HSI=liver weight/eviscerated weight*100 respectively. Biometric data and photographs from a total of 222 sardines were finally collected and used for the analysis (Table 1)

The dimensional characteristics of the swimbladder in each of the aforementioned specimens were studied in more detail by processing the digital images that were collected during the surveys using ImageJ (v. 1.43; http://rsbweb.nih.gov/ij/). Specifically, ventral cross-sectional area of the swimbladder (SB_{xsa}) was measured by spatially calibrating the image using the ruler and by drawing the perimeter of the swimbladder, SB_p. Apart from analyzing its cross-sectional area variability in swimbladder size was also studied by measuring dimensionless shape descriptors such as circularity, aspect ratio, and solidity. Circularity, SB_c, was calculated using the formula:

$$SB_c = \frac{4\pi SB_{xsa}}{\sqrt{SB_p}} \quad (1)$$

A value of 1.0 indicates a perfect circle whilst as the value approaches 0.0 it indicates an increasingly elongated shape. In that respect SB_c together with SB_{xsa} served as indices of inflation (higher values) or deflation (lower values) of the swimbladder. Aspect ratio, SB_{ar}, was the fraction of the major axis divided by the minor axis of the swimbladder. Solidity, SB_s, was calculated using the formula:

$$SB_s = \frac{SB_{xsa}}{SB_{conv}} \quad (2)$$

where SB_{conv} is the convex hull, which can be thought of as a rubber band wrapped tightly around the points that define the selection. As a consequence, SB_s expressed the deviation from normal shapes and the smaller its value the more irregular the outline of the swimbladder.

Among the aforementioned descriptors only SB_{xsa} was significantly related to body size ($P<0.001$). In order to remove this effect and avoid multicollinearity in subsequent analysis due to fish size vs. depth relationship ($P<0.01$) instead of using SB_{xsa} we used the residuals, R, of its allometric relationship with body length ($SB_{xsa} = a * L^b$) (Graham, 2003). The relationship between R, SB_c, SB_{ar}, and SB_s and haul depth was tested using generalized linear models, GLMs. Quantile and residual inspection plots revealed that a Gaussian model with an identity link was the most appropriate for the analysis of R data whilst SB_c, SB_{ar} and SB_s were analyzed using Gaussian models with a logarithmic link. Besides haul depth the

effect of the size of the remaining visceral organs/tissues on swimbladder was also examined. To do so we used HSI, the prevalence of fish with well formed layers of fat surrounding the gut (fat stage >2; see also Silva et al. 2006), P_f, the prevalence of fish with stomachs more than half full (>stage 2 in the scale described by Cunha et al. (2005)), P_s, and the prevalence of females with hydrated ovaries, P_h. Dichotomous P_f, P_s and P_h data were preferable to four or five point scale data because in all cases discrimination between 1 (presence) and 0 (absence) values was performed between the points that reflected the most precipitous change in the size of the respective organ. The selection of the appropriate covariates was performed by stepwise (backward) entry using the Akaike information criterion.

Results

As shown in Figure 2 both cross-sectional area and non-dimensional shape descriptors of the swimbladder were quite variable. Most fish had medium sized swimbladders and in most cases swimbladder had a normal elliptical shape. However, as swimbladder size increased the swimbladder tended to deviate from this normal elliptical shape (Fig. 3). Circularity, SB_c, proved a valid descriptor of swimbladder ventral cross-section since it increased significantly in each swimbladder size class (Fig. 3) and it related significantly with the residuals of the SB_{xsa}-L regression ($P<0.001$; $r^2\approx70\%$). Concerning swimbladder shape descriptors only aspect ratio, SB_{ar}, managed to discriminate normal ellipses from irregular shapes ($P<0.01$; Fig. 2). For solidity, SB_s, normal-elliptical swimbladders did not exhibit significantly different values compared to irregular swimbladders ($P>0.1$; Fig. 2).

Swimbladder size was shown to be related to the depth of capture (ANOVA: $P<0.01$; Fig. 4a). Specifically, fish with smaller swimbladders tended to occur at greater depths. Moreover, using again univariate analysis it was shown that the size of the swimbladder was related with both the reproductive and the feeding state of the individuals. Specifically, hydrated females mainly possessed swimbladders of small or medium size while none of the females with distended swimbladder was hydrated (Fig. 4b). Similarly, the prevalence of fish with filled stomachs declined with increasing swimbladder size and none of the individuals with distended swimbladders had its stomach more than half full (Fig. 4c). Concerning HSI and fat content there was no significant trend with swimbladder size (HSI, ANOVA: $P>0.1$; Fat, Contingency Tables analysis: $P>0.1$).

In GLM analysis the most significant relationship was that between circularity SB_c and haul depth (Table 2, Fig 5). The relationship between R and depth was weaker whilst SB_s was

not related significantly with haul depth (Table 2). The significant positive relationship between SB_{ar} and depth (Table 2) was attributed to the aforementioned finding that deviation from normal shapes was more frequent in larger swimbladders which also mainly occurred at lower depths. From the remaining explanatory factors examined none was shown to significantly affect neither swimbladder size descriptors nor its dimensionless shape descriptors (Table 2). The results concerning the effect of the reproductive state were the same using either GSI or P_h.

Discussion

GLM analysis clearly indicated that swimbladder size in sardine is not affected by the size of other organs inside the coelomic cavity since fish with small ovaries and/or empty stomachs could either have deflated or distended swimbladders. However, taking into account the finite volume of the abdomen, the precipitous changes in swimbladder size from a thin strip to a bulbous sac and the transient changes in size that most of the visceral organs undergo it might be postulated that the inverse situation is quite possible, i.e. swimbladder size determining the size of some organs inside the coelomic cavity. Indeed, the decrease in the proportion of fish with hydrated ovaries or filled stomachs with increasing swimbladder size and more importantly the complete absence of these reproductive/feeding states in fish with distended swimbladders indicate that swimbladder size might have an adoptive or functional relationship with these two organs. For instance, in fish with distended swimbladders the excess of food could be evacuated due to limitations in stomach volume inside the restricted coelomic cavity.

On the other hand the relationship between swimbladder size and reproductive state might be of more adoptive nature. Gonad size in sardine is known to undergo significant changes during the spawning cycle with its most striking increase taking place at oocyte hydration just previous to spawning (Somarakis et al., 2004); from simple macroscopic observation it might be inferred that a pair of fully hydrated ovaries would be hard to co-occur with a bulbous swimbladder inside the coelomic cavity. In that respect it might be postulated that spawning at a depth where swimbladders are deflated provides more space for hydration to occur and for ovaries to develop. Indeed, there is strong evidence that imminent spawning sardines separate spatially from the remaining population to formulate ephemeral spawning aggregations in deeper layers (Ganias, 2008).

Another interesting result which shows that swimbladder is rather the explanatory than a dependent factor in the competition for space among the visceral organs is that its size was shown to be related only with organs that undergo transient changes (stomach: diurnal changes; gonads: daily, diurnal changes) and not with liver and fat which fluctuate at a rather seasonal scale (Nunes et al., 2009). If swimbladder size was subtle to deflation from an increasing internal pressure due to turgid organs then fish with large liver or higher fat reserves would display smaller swimbladders but present analysis did not demonstrate the existence of this relationship.

On the other hand, sampling in our study took place inside sardine spawning season which is a period of fat depletion and thus the effect of high amounts of visceral fat (i.e. summer; Nunes et al., 2009) could not be evaluated. For instance, in their laboratory study Machias & Tsimenides (1995) used seasonal collections of Mediterranean sardine, *S. pilchardus*, to show that swimbladder size is smaller in individuals of higher lipid content.

Depth related changes in swimbladder size have already been described for herring (Blaxter et al., 1979; Ona, 1990) and are postulated to occur in other physostomous clupeoids too like the Japanese anchovy, *Engraulis japonicus* (Zhao et al., 2008). Thus, whatever the actual nature of the above relationships among different visceral compartments, the present study managed to provide a rather simplistic and cost-effective means for demonstrating bathymetric adjustment in the swimbladder of a physostomous clupeid which in turn validates its use. There are good reasons to believe that our measurements were accurate. Blaxter et al. (1979) suggested for freshly caught herring that gas loss through the swimbladder was impossible without activating the voiding reflex via the anal duct whilst gas uptake due to swallowing air at the surface as fish were brought on-board was also unlikely to happen. In the present study, sardine swimbladder size was not related to the duration of the hauls which suggests that the effect of the sheer physical process of trawling and hauling on swimbladder size was either absent or equal among different hauls. Thus, even if our measurements took place at the sea surface after the fish have been stuck and squashed in the codend, variability in swimbladder size was not related with the duration of the hauling process. Furthermore, Robertson et al. (2008) showed for another physostomous teleost, the zebrafish *Danio rerio*, that swimbladder size in dissected specimens did not differ significantly from *in-situ* X-Ray measurements which indicates that our anatomy scheme which involved slitting and opening of the coelomic cavity should not have affected swimbladder size.

The Atlantic sardine is a pelagic fish that performs extended diurnal vertical migrations (Zwolinski et al., 2007). As acoustic surveys are often operated on a 24-h basis, the observed depth-dependence of swimbladder size may have direct effect on fish target-strength, TS, and consequently on the resulting biomass estimates. Similar results for depth dependence of TS were provided by Zhao et al. (2008) for the Yellow Sea anchovy, *E. japonicus*; the authors further suggested that TS values would be elevated by 2 dB when fish migrate from 50 m deep during daylight to 20 m deep at night resulting in a 58% difference between daytime and nighttime biomass estimates. In that respect our method may provide an easy means for measuring swimbladder size in parallel with body size measurements in acoustic surveys in order to make the appropriate calibrations in the analysis of backscaterring energy.

Acknowledgments

The present work was operated within the framework of IPIMAR's acoustic surveys funded by the by the Portuguese sampling program integrated in the EU Data Collection Regulation. Stella Michou is thanked for technical assistance contributing to the measurement of swimbladder cross-sections. Drs Cristina Nunes, Yorgos Stratoudakis, and Dr. Alexandra Silva are greatly thanked for providing help at various steps of this work and D. Morais is thanked for the acquisition of sardine biological data during the cruises.

References

Blaxter, J. H. S.; Denton, E. J.; Gray, J. A. B., 1979: The herring swimbladder as a gas reservoir for the acousticolateralis system. J. Mar. Biol. Ass. U.K. **59**, 1-10.

Cunha, M. E.; Garrido, S.; Pissarra, A., 2005: The use of stomach fullness and colour indices to assess *Sardina pilchardus* feeding. J. Mar. Biol. Ass. U.K. **85**, 425-431.

Fine, M. L.; McKnight Jr., J. W.; Blem, C. R., 1995: Effect of size and sex on buoyancy in the oyster toadfish. Mar. Biol. **123**, 401-409.

Foote, K. G., 1980: Importance of the swimbladder in acoustic scattering by fish: A comparison of gadoid and mackerel target strengths. J. Acoust. Soc. Am. **67**, 2084-2089.

Ganias, K., 2008: Ephemeral spawning aggregations in the Mediterranean sardine, *Sardina pilchardus*: a comparison with other multiple-spawning clupeoids. Mar. Biol. **155**, 293-301.

Graham, M. H., 2003 Confronting multicollinearity in ecological multiple regression. Ecology **84**, 2809-2815.

Machias, A.; Tsimenidis, N., 1995: Biological factors affecting the swimbladder volume of sardine (*Sardina pilchardus*). Mar. Biol. **123**, 859-867.

Nero, R.; Thompson, C.; Jech, J., 2004 In situ acoustic estimates of the swimbladder volume of Atlantic herring (*Clupea harengus*). ICES J. Mar. Sci. **61** 323-337.

Nunes, C.; Silva, A.; Ganias, K., 2009: Seasonality of the reproductive activity and resources allocation in the Iberian sardine. 4th Workshop on Gonadal Histology of Fishes 16-19 June 2009, El Puerto de Santa María, Cádiz, Spain.

Ona, E., 1990: Physiological factors causing natural variations in acoustic target strength of fish. J. Mar. Biol. Ass. U.K. **70**, 107-127.

Robertson, G. N.; Lindsey, B. W.; Dumbarton, T. C.; Croll, R. P.; Smith, F. M., 2008 The contribution of the swimbladder to buoyancy in the adult Zebrafish (*Danio rerio*): A morphometric analysis. J. Morphol. **269**, 666-673

Silva, A.; Santos, M.; Caneco, B.; Pestana, G.; Porteiro, C.; Carrera, P.; Stratoudakis, Y., 2006: Temporal and geographic variability of sardine maturity at length in the northeastern Atlantic and the western Mediterranean. ICES J. Mar. Sci. **63**, 663-676.

Somarakis, S.; Ganias, K.; Tserpes, G.; Koutsikopoulos, C., 2004: On gonadal allometry and the use of the gonosomatic index: a case study in the Mediterranean sardine, *Sardina pilchardus*. Mar. Biol. **146**, 181-189.

Zhao, X. Y.; Wang, Y.; Dai, F. Q., 2008: Depth-dependent target strength of anchovy (*Engraulis japonicus*) measured in situ. ICES J. Mar. Sci. **65**, 882-888.

Zwolinski, J.; Morais, A.; Marques, V.; Stratoudakis, Y.; Fernandes, P. G., 2007: Diel variation in the vertical distribution and schooling behaviour of sardine (*Sardina pilchardus*) off Portugal. ICES J. Mar. Sci. **64**, 963-972.

Figure legends

Figure 1. Ventral views of sardines with the abdomen opened to expose the swimbladder. Left panel illustrates variability in size among swimbladders with normal-elliptical shape: (a) small; (b) medium; (c) large; (d) distended. Right panel illustrates variability in shape in swimbladders with large size: (e) compressed medially; (f) compressed at the anterior region; (g) compressed at the posterior region. The head is always to the right.

Figure 2. Frequency distribution of sardine swimbladders at each size (left panel) and shape (right panel) class and means plots of the residuals of SB_{xsa}-L relationship, R, and circularity, SB_c, at each size class and of aspect ratio, SB_{ar}, and solidity, SB_s, at each shape class. Homogeneous groups (95%, LSD multiple range test) are marked with identical symbols. Vertical bars correspond to 95% confidence intervals.

Figure 3. *Sardina pilchardus*. Breakdown of each swimbladder size class (1: small; 2 medium; 3; large; 4: distended) into shape classes (legend on the right, 1: normal-elliptical; 2 medially compressed; 3; compressed at the anterior region; 4: compressed at the posterior region).

Figure 4. *Sardina pilchardus*. Average depth, prevalence of hydrated females, P_h, and prevalence of fish with stomachs more than half full, P_s, in each swimbladder size class. Vertical bars in plot (a) represent 95% confidence intervals. Dotted horizontal lines in plots (b) and (c) represent 95% decision limits, whilst asterisks in the same plots represent proportions that differ significantly from the average (solid horizontal line).

Figure 5. *Sardina pilchardus*. Component effect of haul depth on the circularity of sardine swimbladders as derived from GLM analysis.

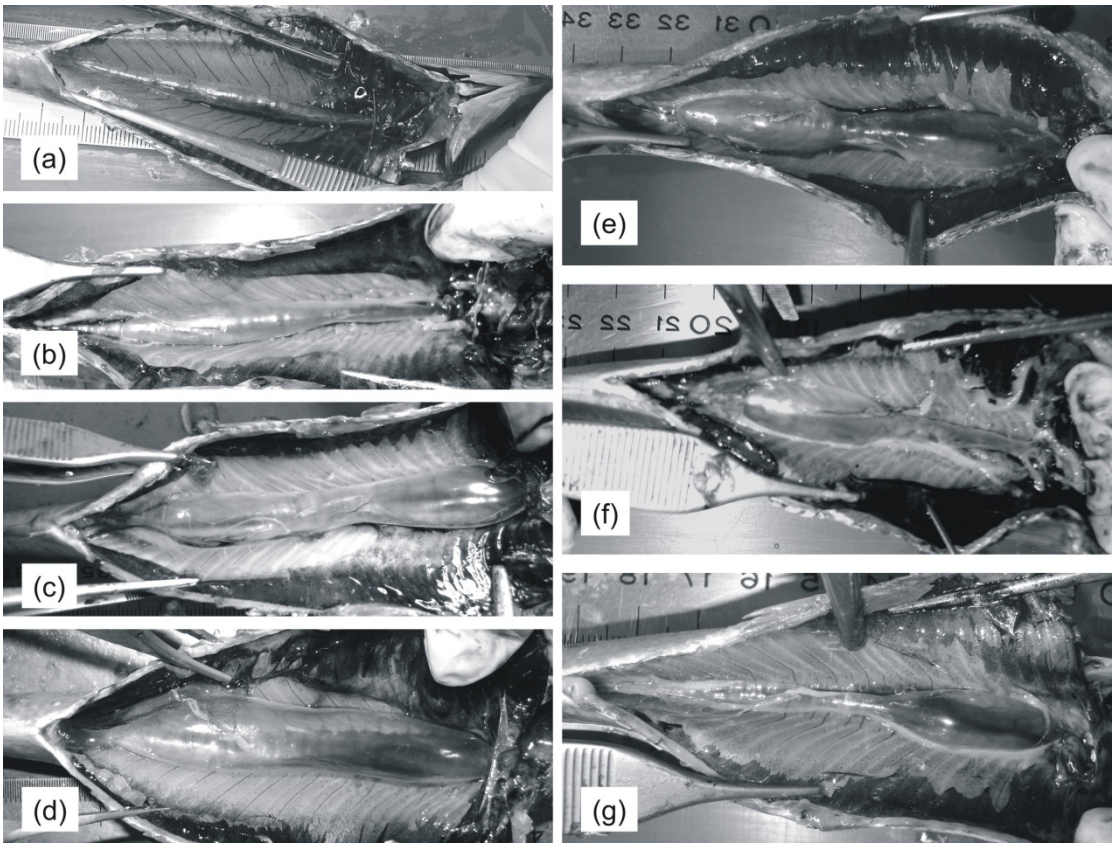

Ganias et al. Figure 1

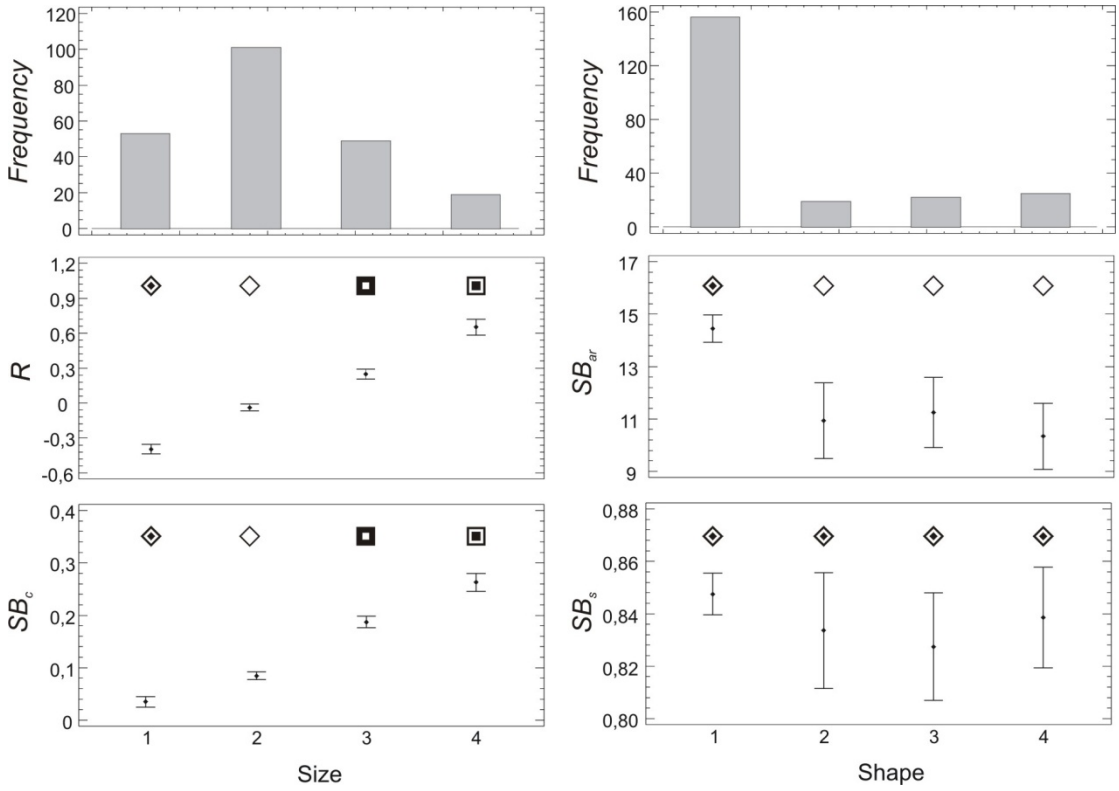

Ganias et al. Figure 2

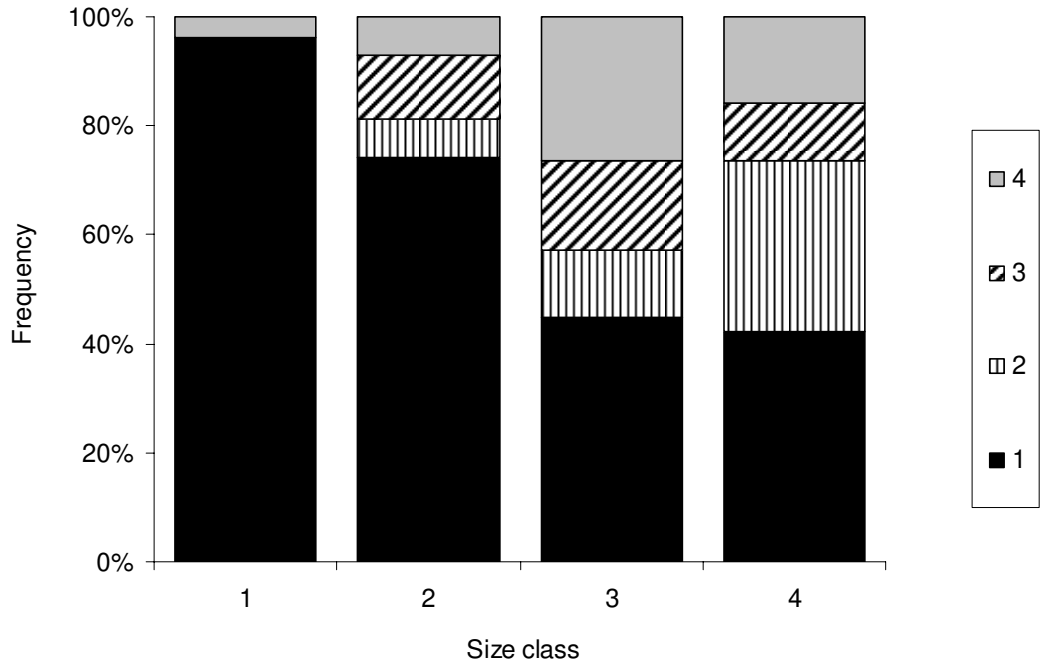

Ganias et al. Figure 3

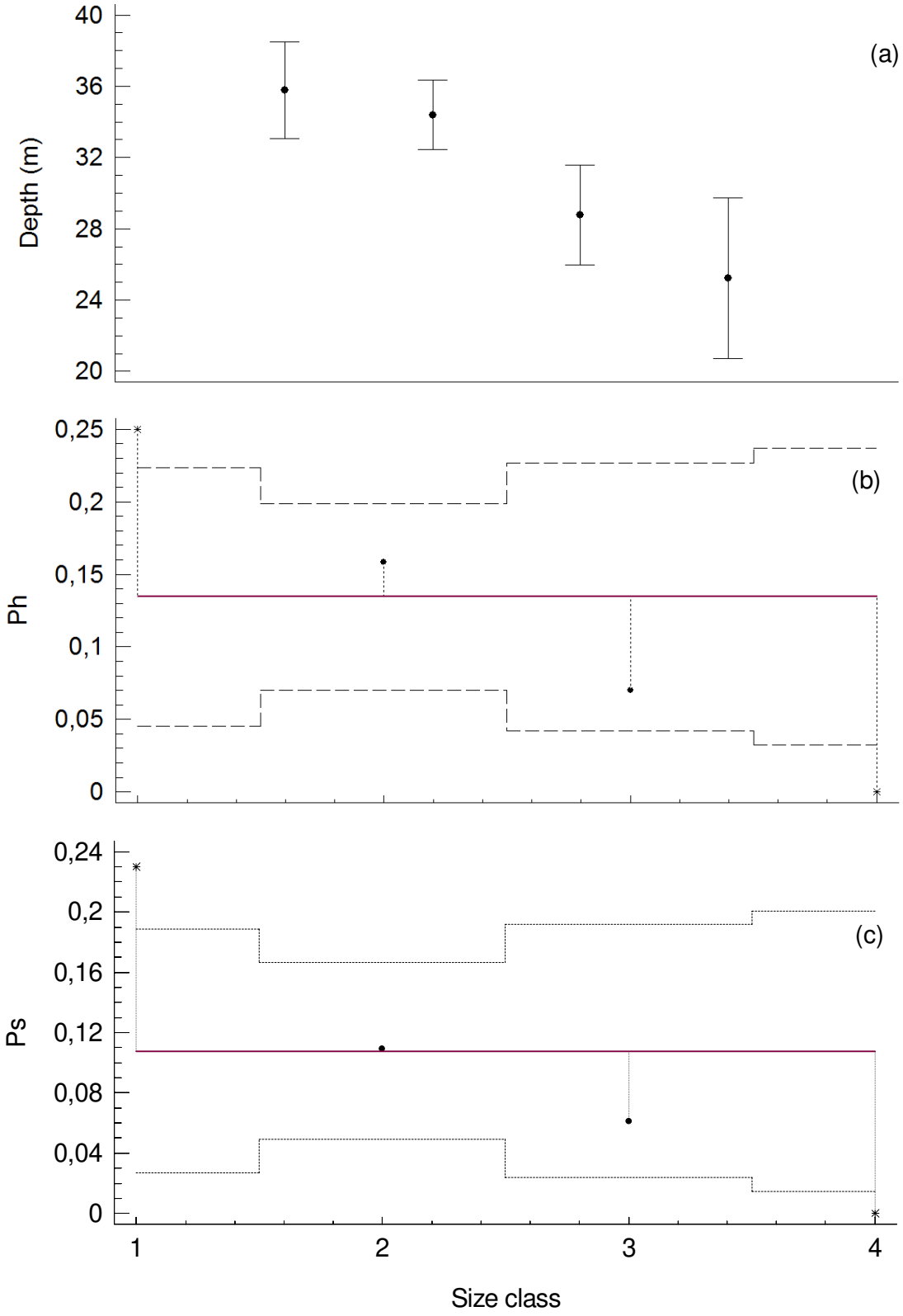

Ganias et al. Figure 4

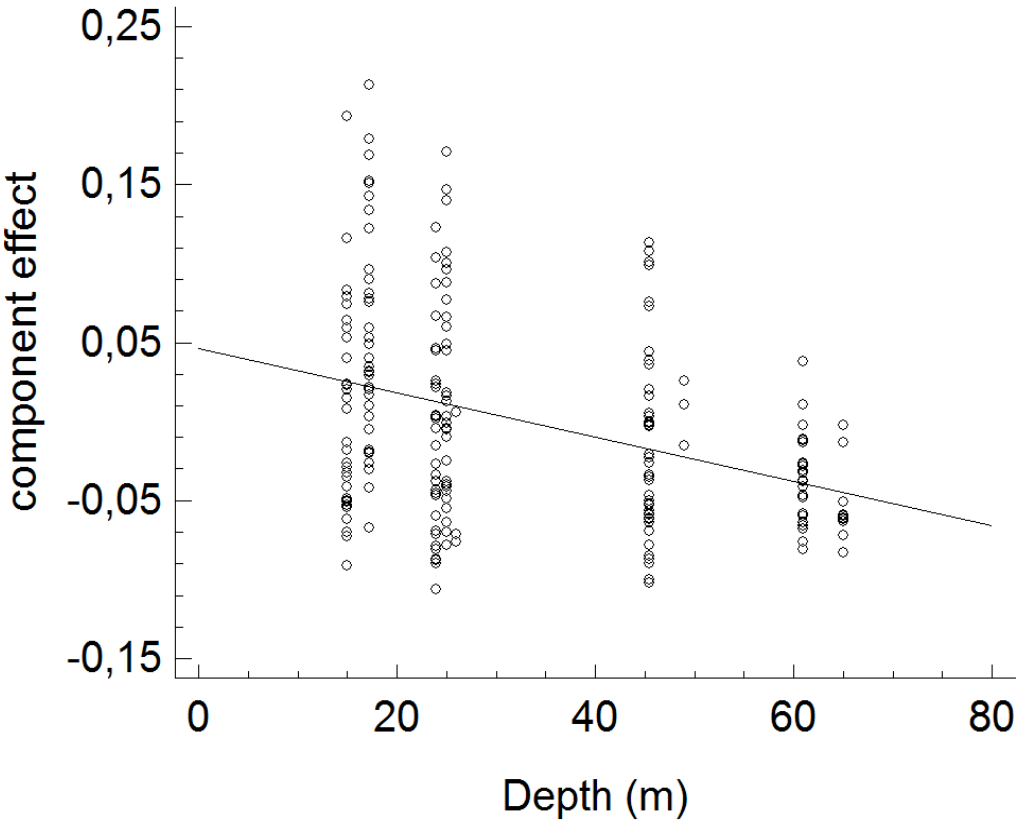

Ganias et al. Figure 5

372 **Table 1**. Characteristics of the ten samples used to measure biometric data and swimbladder size and
373 shape of sardine, *Sardina pilchardus*. n: number of fish analyzed; *L*: average length (cm); SB_{xsa}:
374 average swimbladder ventral cross-section (cm^2). Minimum and maximum values are provided in
375 parentheses.

Sample	*Date*	*Time*	*Average haul depth*	*n*	*L*	SB_{xsa}
1	18/10/2008	9:20	25,0	29	20,1	4,14
					(18,2-22,2)	(0,70-9,46)
2	19/10/2008	13:45	17,3	39	20,3	5,54
					(19-22,7)	(1,80-12,11)
3	20/10/2008	16:15	24,0	31	18,3	2,97
					(14,7-20,6)	(1,13-5,87)
4	21/10/2008	8:45	45,5	45	19,1	3,77
					(18,0-20,3)	(1,92-7,50)
5	24/10/2008	13:50	15,0	33	19,5	4,05
					(18,5-20,4)	(1,95-7,66)
6	3/4/2009	17:20	65,0	11	19,9	3,03
					(17,5-21,2)	(2,27-4,17)
7	1/4/2009	17:08	61,0	26	19,5	2,81
					(17,6-21,4)	(1,60-4,64)
8	16/4/2009	15:57	26,0	3	18,9	2,28
					(18,3-19,7)	(1,19-3,36)
9	18/4/2009	15:07	49,0	3	19,4	4,71
					(19,2-19,7)	(4,45-4,97)
10	21/4/2009	18:38	25,0	2	21,5	5,02
					(21,2-21,8)	(3,71-6,33)

376

Table 2. Coefficients of the models used to analyze the effect of depth, prevalence of hydrated gonads, P_h, prevalence of stomachs more than half full, P_s, prevalence of well formed fat strips, P_f, and hepatosomatic index HSI on sardine swimbladder size and dimensionless shape descriptors. *R*: residuals of the relationship between swimbladder ventral cross-section and body length; SB_c: swimbladder circularity; SB_{ar}: swimbladder aspect ratio; SB_s: swimbladder solidity.

Source of variation	***R***	***SB*$_c$**	***SB*$_{ar}$**	***SB*$_s$**
Null	0.061*	-1.318**	2.465	-0.134**
Depth	-0.003*	-0.008**	0.005**	*ns*
P_h	*ns*	*ns*	*ns*	*ns*
P_s	*ns*	*ns*	*ns*	*ns*
P_f	*ns*	*ns*	*ns*	*ns*
HSI	*ns*	*ns*	*ns*	*ns*

ns: non significant; *: 0.05>*P*>0.01, **: *P*<0.01